Journal of Fluorescence (2019) 29:1349–1358
https://doi.org/10.1007/s10895-019-02462-5

ORIGINAL ARTICLE

An Application of a Schiff-Base Type Reaction in the Synthesis of a New Rhodamine-Based Hg(II)-Sensing Agent

Fulya Cicekbilek[1] · Bahar Yilmaz[1] · Mevlut Bayrakci[1] · Orhan Gezici[2]

Received: 8 July 2019 / Accepted: 5 November 2019 / Published online: 13 November 2019

Abstract

A facile synthesis procedure, whereby 9-Anthraldehyde (AA) is coupled to aminated rhodamine (AR) via a Schiff base-type reaction, is reported. The applicability and performance of the obtained material (AA-AR) as a sensing agent was studied towards 16 metal cations (i.e. Li^+, Na^+, Ag^+, Ca^{2+}, Ba^{2+}, Co^{2+}, Cs^+, Cu^{2+}, Mg^{2+}, Hg^{2+}, Mn^{2+}, Pb^{2+}, Ni^{2+}, Sr^{2+}, Zn^{2+}, Al^{3+}). Among the studied metals, an extraordinary selectivity was observed for Hg^{2+}, and the observed selectivity was found not to be influenced by the presence of other cations and some common anions (i.e. Br^-, Cl^-, I^-, HPO_4^{2-}, $H_2PO_4^-$, NO_3^-, NO_2^-, ClO_4^-, AcO^-, HSO_4^-, SO_4^{2-}, $Cr_2O_7^-$, CO_3^{2-}, OH^- and HCO_3^-). The material, AA-AR, exhibited such a high selectivity and sensitivity towards Hg^{2+} that it could be detected even by naked eyes. The Hg^{2+}-sensing property of AA-AR was found not to be limited to colorimetric detections so that a high fluorescent nature of the compound was also observed upon binding Hg^{2+} ion. The detection limit, which is correspondent to fluorescence emission intensity, was found as 0.87 μM. The underlying mechanism of sensing property was studied by using some spectroscopic techniques such as FT-IR, ^{1}H-NMR, ^{13}C-NMR, and UV-Vis. (Job-plot). In the final course of the experiments, the performance of AA-AR in cell-imaging was also studied, and even trace amounts of Hg^{2+} in living cells could be detected by the studied probe. Thus, the applicability of a new synthesis approach in producing a highly efficient new fluorescence sensor for the detection of Hg^{2+} ions is discussed in detail.

Keywords Anthracene · Cell imaging · Fluorescence sensor · Mercury · Rhodamine · Schiff base

Introduction

Fluorescence sensing techniques have received great interest from different disciplines over the past decades. Together with the selectivity and sensitivity achieved with these techniques, they offer easy-to-use, inexpensive, fast, flexible, and innovative analytical perspectives [1–3]. Hence, the fluorescence sensing techniques comprise a series of detection manners that are, today, indispensable for analytical chemists when fast, selective and sensitive detection of a chemical or a biologically-important species is necessary.

✉ Mevlut Bayrakci
mevlutbayrakci@gmail.com

✉ Orhan Gezici
ogezici@gmail.com; ogezici@ohu.edu.tr

[1] Faculty of Engineering, Department of Bioengineering, Karamanoglu Mehmetbey University, Karaman, Turkey

[2] Faculty of Science and Arts, Chemistry Department, Nigde Ömer Halisdemir University, 51240 Nigde, Turkey

The sensing agent (i.e. fluorescence sensor) is a chemical that is prepared by combining "a receptor" with "a fluorophore" by chemical means, and it is, actually, the key factor that determines the overall success of a fluorometric sensing technique. For this reason, nowadays, greater emphasis is given to the development of new types of sensing agents exposing high selectivity and sensitivity toward the chemical species under consideration. With this regard, intelligent design and synthesis of a sensing agent is, admittedly, an art of science that requires a collective knowledge of chemistry and spectroscopy. In the past decades, many different fluorescence sensors were developed due to the potential of this technique in different fields ranging from environmental sciences to medicine [4–6].

Detection of heavy metal ions in various environments is one of the most widely studied fields where the fluorescence sensing techniques applied successfully. With this respect, simplicity, high selectivity, low operation costs, and (sometimes) the possibility of naked-eye detection are some advantages of fluorescence sensing techniques over much more sophisticated instrumental techniques. Among the heavy

metals, mercury is a highly toxic one since it can readily penetrate through the cell membranes because of its solubility in the lipid bilayer [7, 8]. Thus, mercury ions are recognized as a primary source of health problems for living things even at trace levels [9, 10]. For this reason, selective, sensitive, and rapid detection of mercury ions in various media is deemed important. Several analytical techniques such as voltammetry, atomic-absorption spectroscopy (AAS), inductively coupled plasma emission spectroscopy (ICP-AES), and potentiometric and spectrophotometric sensors have been utilized to detect trace levels of mercury ions [11–15]. Despite their widespread use, some of the mentioned techniques are generally labor-intensive, and expensive when compared to fluorescence sensing techniques. Moreover, their selectivity is usually less than that achieved with the fluorometric techniques [16].

Rhodamine-based sensors have been widely used in sensing applications of metal ions. This is, basically, due to high quantum yields and high molar extinction coefficients achieved with rhodamine-based agents. Good photostability, and relatively long absorption and emission wavelengths are some other advantages of this class of sensors [17]. Because of these properties, rhodamine-based sensors exhibit strong color shifts upon interaction with chemical species which sometimes provide "naked-eye" detection of ions. As it is seen in the literature, the applicability of rhodamine-based agents as fluorescence sensors for the determination of mercury ions is an extensively studied topic [5, 6, 17]. It should, however, be noticed that only a limited number of the studied sensors have exhibited high sensitivity and selectivity toward mercury ions. In order to increase the efficiency and the stability of rhodamine-based sensors, some researchers have studied the incorporation of sulfur-containing groups into the rhodamine framework [18–20]. However, the presence of sulfur in the prepared sensors can constitute serious problems for living things, and therefore, alternative –safer– strategies are necessary to prepare rhodamine-based sensors.

Schiff-base type reactions offer easy, mild and sometimes one-step manners in the synthesis of functional materials. Therefore, a Schiff-base type reaction might be a method of choice when preparing Hg^{2+}-selective rhodamine-derivatives. Except few attempts [21], the applicability of this approach is seen to be lacking in the literature whereas it is promising to build highly selective, sensitive and biocompatible rhodamine-based Hg^{2+} sensors. Thus, in the present study, we focus on the applicability of a straightforward Schiff-base-type condensation reaction between aminated rhodamine (AR) and antraldehyde (AA) to prepare a rhodamine-anthracene chemosensor for the first time. Both characterization of the prepared material and its sensor properties have been critically drawn throughout the work.

Materials and Methods

Chemicals and Instruments

Rhodamine B, 9-Anthracenecarboxaldehyde, and the studied metal salts were of analytical grade and used as received (Sigma-Aldrich). Nitrate salts of some common cations (i.e. Li^+, Na^+, Ag^+, Ca^{2+}, Ba^{2+}, Co^{2+}, Cs^+, Cu^{2+}, Mg^{2+}, Hg^{2+}, Mn^{2+}, Pb^{2+}, Ni^{2+}, Sr^{2+}, Zn^{2+} and Hg^{2+}), and tetra butyl ammonium salts of some common anions (i.e. Br^-, Cl^-, I^-, HPO_4^{2-}, $H_2PO_4^-$, NO_3^-, NO_2^-, ClO_4^-, AcO^-, HSO_4^-, SO_4^{2-}, $Cr_2O_7^-$, CO_3^{2-}, OH^- and HCO_3^-) were used to prepare synthetic test solutions in DMF (Merck).

^{1}H-NMR and ^{13}C-NMR spectra were generated by an Agilent™ Premium Compact spectrometer operating at 600 MHz. A Bruker™ Vertex FTIR spectrophotometer with an ATR compartment was used for recording FTIR spectra. UV-Vis. absorption spectra were collected on a Shimadzu™ UV-1800 instrument, and the fluorescence measurements were conducted on a Hitachi™ F-7100 instrument.

Fresh ultrapure water produced on a Millipore™ Milli-Q Plus water purification system was used throughout the study.

Synthesis and Characterization of the Sensing Agent (AA-AR)

Aminated-rhodamine (AR) was synthesized according to a known procedure [22]. A 75 mM solution of AR was prepared in ethanol, and 1.0 eq of 9-Anthraldehyde (AA) was added to 20.0 mL of this solution while stirring the mixture, continuously. The final mixture was stirred overnight under reflux. Afterward, the solvent was evaporated under vacuum, and the solid residue was, subsequently, washed with 1.0 M HCl, brine and water. The crude product (AA-AR) was crystallized from hot methanol. The product, which is a dark-red solid, was obtained with a 56% yield, and the molecular structure was confirmed with FTIR, NMR, and elemental analysis techniques. A summary of the synthesis procedure is given in Scheme 1.

Absorption and Fluorescence Measurements

Before spectrophotometric measurements, the stock solutions which comprise (*i*) a 1.0 mM AA-AR solution, (*ii*) 1.0 mM solutions of metal cations, and (*iii*) 1.0 mM solutions of anions were prepared (in DMF). Test solutions were prepared by the addition of 20 eq cation or anion to 0.010 mM AA-AR solution, and the final volume was fixed at 2.0 mL. The absorption spectra of AA-AR with and without studied ions were recorded in the range of 200–600 nm using a UV-Vis. spectrophotometer. The emission spectra were recorded at room temperature and the instrument parameters were set as follows: Excitation wavelength (λ_{ex}: 520 nm; scan speed: 1200 nm/

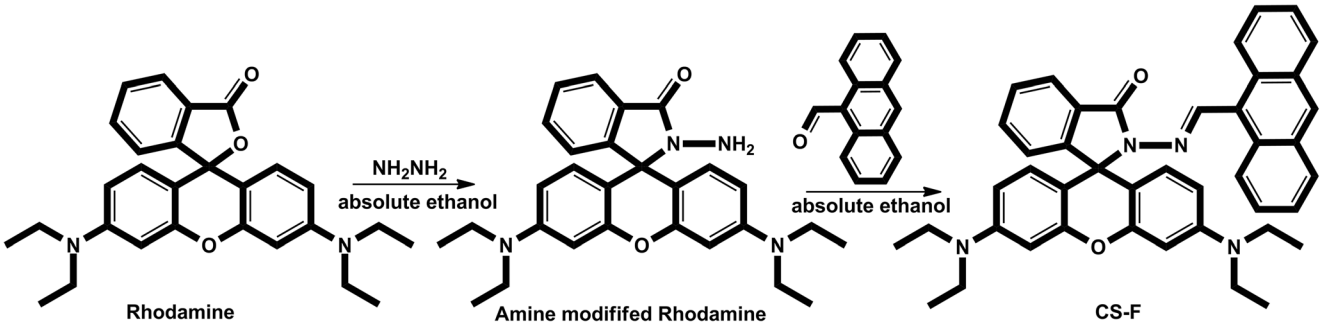

Scheme 1 A schematic view for the synthesis of AA-AR probe

min; PMT voltage: 400 V; Emission wavelength scan range: 540–750 nm; and slit width: 10 nm (both for excitation and emission). During the fluorescence intensity measurements, the excitation (λ_{ex}) and the emission (λ_{em}) wavelengths were set at 520 and 592 nm, respectively.

Cell Imaging

The living cells of MCF7 and MIA PaCa-2 were supplied from ATCC (American Type Culture Collection, Rockville, MD, USA). The cells were incubated in a Hg^{2+} solution of 0.010 mM in the culture medium at 37 °C for 1 h. After washing the cells with phosphate-buffered saline (PBS), 0.020 mM AA-AR was added to the medium just before cell-imaging. Bright-field and fluorescent images were taken by using a Leica™ DM3000 fluorescence microscopy.

Results and Discussion

Characterization of AA-AR

The studied approach, which is based on a Schiff-base-type reaction, yielded a dark-red solid, i.e. AA-AR, with a 56% yield. The molecular structure of the product was studied by various techniques like elemental analysis, FTIR, ^{1}H-NMR and ^{13}C-NMR spectroscopy analyses.

The results of elemental analysis perfectly fitted to the theoretical atomic percentages we expected for AA-AR, and thus confirming the molecular formula $C_{43}H_{40}O_2N_4$:

- Theoretical atomic percentages ➔ C: 80.10%; H: 6.25%; N: 8.69%.
- Experimental atomic percentages ➔ C: 80.13%; H: 6.29%; N: 8.62%.

Further information about the molecular structure was gathered from FTIR spectroscopy analysis. The following basic vibration bands, which confirm the molecular structure, were seen in the FTIR spectrum of AA-AR (Fig. 1):

- 2964 cm^{-1} (Aromatic C–H stretching);
- 2900–2925 cm^{-1} (Aliphatic C–H stretching);
- 1683 cm^{-1} (C=O stretching vibration for amides);
- 1631 cm^{-1} (C=N, for azomethine moiety);
- 1548–1413 cm^{-1} (C=C vibrations).

In order to have more details about the structure, ^{1}H-NMR and ^{13}C-NMR analyses were also conducted, and the results are listed below (Fig. 2):

- ^{1}H NMR (600 MHz $CDCl_3$): δ 8.31 (s, 1H, CH=N), 8.06 (s, 1H, Ar-H), 8.00–7.99 (d, J = 8.6 Hz, 2H, Ar-H), 7.88–7.86 (d, J = 8.2 Hz, 2H, Ar-H), 7.53–7.50 (m, 3H, Ar-H), 7.36–7.30 (m, 2H, Ar-H), 7.29–7.25 (m, 2H, Ar-H), 7.21–7.20 (d, 1H, J = 8.4 Hz, Ar-H), 6.77–6.75 (d, 2H, J = 8.7 Hz, Ar-H), 6.47 (s, 2H, Ar-H), 6.36–6.35 (d, 2H, J = 8.8 Hz, Ar-H), 3.34–3.33 (m, 8H, $\underline{CH_2}$-CH_3), 1.15–1.14 (m, 12H, CH_2-$\underline{CH_3}$).
- ^{13}C NMR ($CDCl_3$): δ 165.12, 152.97, 152.22, 149.02, 147.08, 133.45, 131.15, 129.92, 128.76, 128.38, 127.92, 127.69, 126.18, 125.53, 125.01, 123.81, 123.53, 108.26, 105.95, 98.29, 65.82, 44.35, 12.64.

Absorption and Emission Behavior of AA-AR

The Impact of Hg^{2+}

Since developing a new sensing agent for Hg^{2+} constitutes the objective of the present work, after synthesis and characterization of AA-AR, we directly focused on the effect of Hg^{2+} on absorption and emission spectra of AA-AR, as spectral changes could guide us to have some intuitions about the potential of the new material as a sensor. For this purpose, a solution of AA-AR (0.010 mM; in DMF) was spiked with different amounts of Hg^{2+} ranging from 0.0 to 20.0 eq, and both absorption and emission spectra were recorded (Figs. 3 and 4).

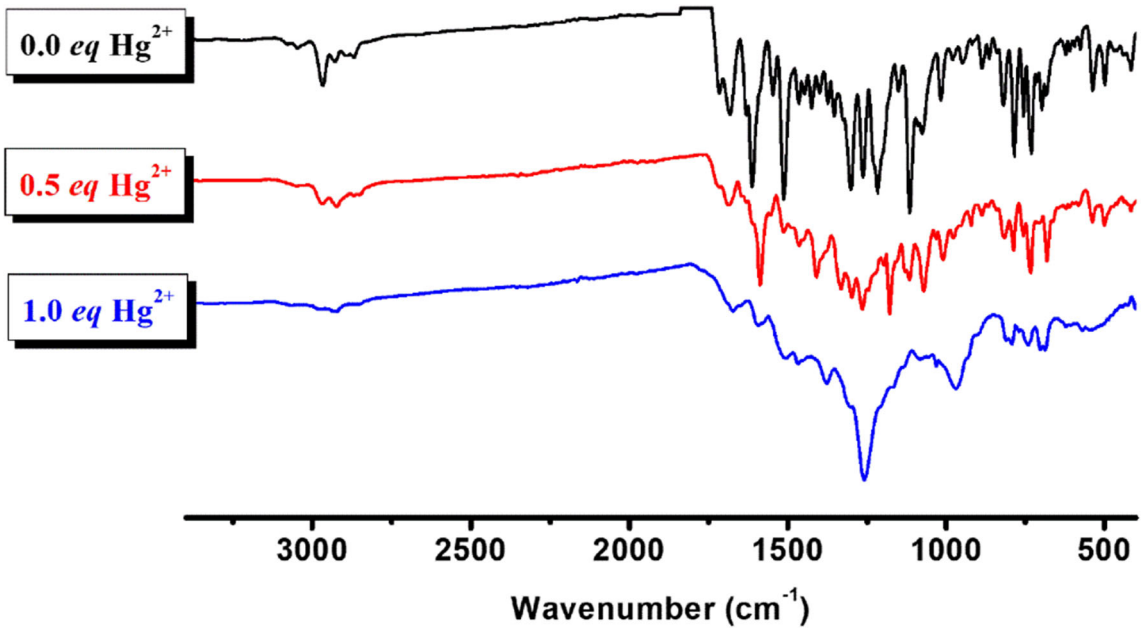

Fig. 1 FTIR spectra for AA-AR (i.e. 0.0 eq Hg^{2+}) and AA-AR-Hg^{2+} (0.5 eq and 1.0 eq)

As seen in Fig. 3, the absorption spectrum of AA-AR comprises two broad absorption bands at around 315 and 400 nm. Intra-ligand $\pi-\pi^*$ charge transfer electronic transitions resulting from anthracene moiety (coupled to rhodamine molecule) was thought to be the main source of these bands. Though very weak, a band centered at around 560 nm was also observed in the spectrum of AA-AR. Surprisingly, the intensity of this band was observed to be increased immediately after interacting AA-AR molecule with Hg^{2+} ion, and higher Hg^{2+} concentrations resulted in greater intensities at this wavelength. Despite such an obvious change in the absorption intensity at 560 nm, the addition of Hg^{2+} ion has no significant impact on the intensities of the bands at 315 and 400 nm as is seen in Fig. 3. Thus, AA-AR was found to be absorbing in the UV and visible regions, and the intensity of the absorption at 560 nm was understood to be affected by the concentration of Hg^{2+}.

When we come to the emission spectra recorded for AA-AR, up to 37-fold increment in fluorescence intensity could be achieved when the probe interacted with Hg^{2+} ion (Fig. 4). This revealed a high fluorescence character of the AA-AR-Hg^{2+} complex at 592 nm when it is excited at 520 nm. All these observations implied the potential of AA-AR as a sensing agent for Hg^{2+}. However, most of the discussions would remain as speculative, without studying the selectivity of AA-AR toward Hg^{2+}. Thus, after studying the general absorption and emission behavior of AA-AR probe with respect to the spectral changes after its interaction with Hg^{2+} ion, in the second part of the study, we, basically, focused on the influence of various metal cations and some common anions on the absorption and the emission behavior of the probe.

The Impact of some Common Cations and Anions

Single-solute experiments performed with Hg^{2+} revealed a nice sensor property toward this highly toxic ion. However, without analyzing the effect of some common cations and anions, this observed sensor property would remain as unproven and most of the discussions would be speculative. With this sense, the spectral pattern of ion-interacted AA-AR was studied with respect to 16 metal cations (i.e. Li^+, Na^+, Ag^+, Ca^{2+}, Ba^{2+}, Co^{2+}, Cs^+, Cu^{2+}, Mg^{2+}, Hg^{2+}, Mn^{2+}, Pb^{2+}, Ni^{2+}, Sr^{2+}, Zn^{2+}, Al^{3+}) and 15 common anions (i.e. Br^-, Cl^-, I^-, HPO_4^{2-}, $H_2PO_4^-$, NO_3^-, NO_2^-, ClO_4^-, AcO^-, HSO_4^-, SO_4^{2-}, $Cr_2O_7^-$, CO_3^{2-}, OH^- and HCO_3^-).

Among the studied cations, Hg^{2+} was the only one that had a considerably high impact on the absorption spectra of AA-AR. As it is discussed above, the greatest change in the spectrum of AA-AR was recorded at 560 nm after its interaction with Hg^{2+}. Hence, in the case of other studied cations and anions, no considerable change was observed in the spectrum of AA-AR regardless of the type of ion. Note that some weak hyperchromic and/or hypochromic changes centered at around 315 nm and 400 nm could be observed with some ions (Figures not shown).

As it is well known, absorption and emission spectroscopies are complementary techniques in evaluating the sensor property of a probe. It should, however, be noticed that the fluorescence emission spectroscopy offers much better selectivity as well as sensitivity, and thus becoming an indispensable technique in sensor applications. In this regard, the fluorescence emission spectra for ion-interacted AA-AR were also analyzed, and the spectra recorded for single-solute samples were compared with that of AA-AR-Hg^{2+} (Fig. 5).

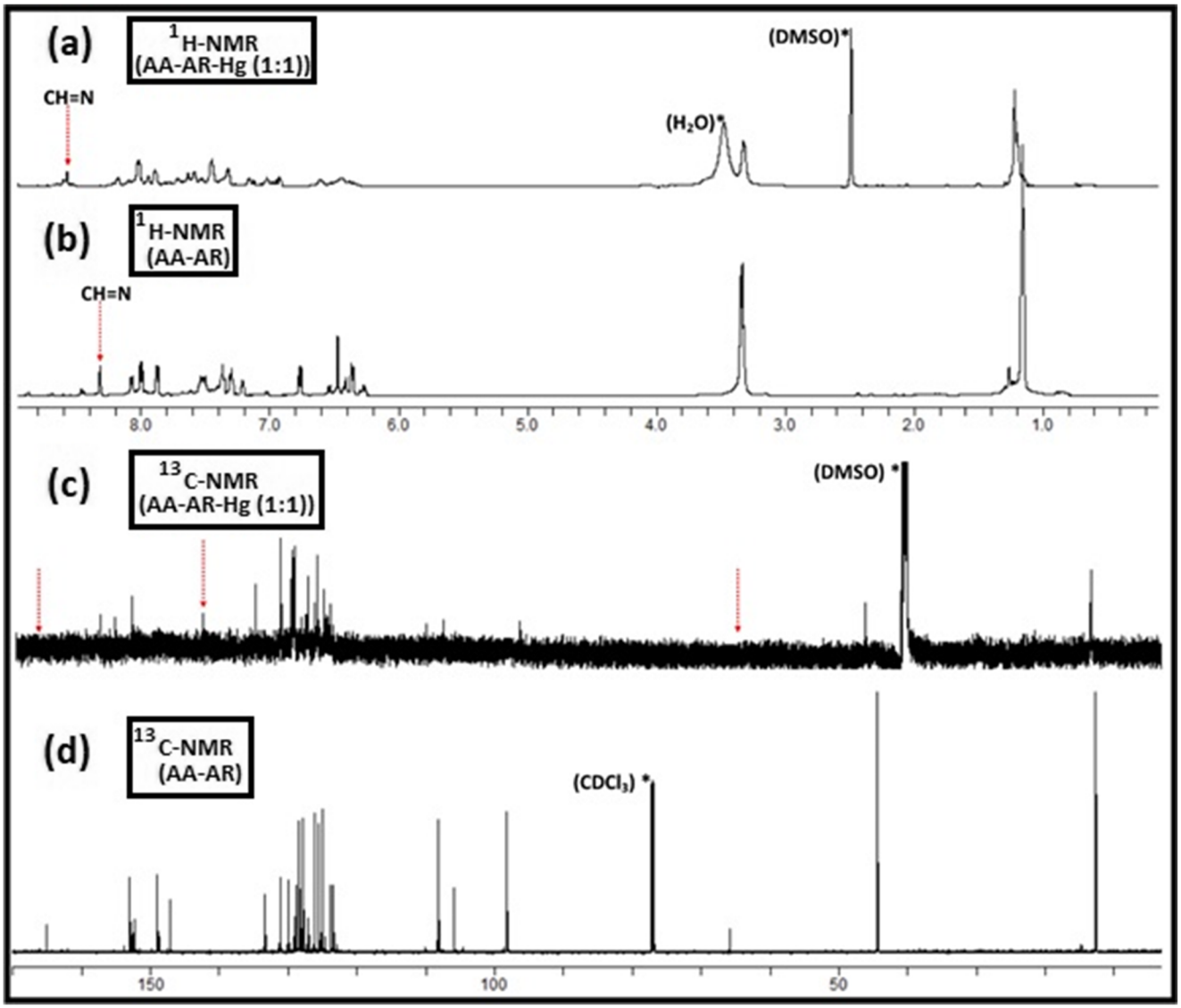

Fig. 2 ^{1}H-NMR and ^{13}C-NMR spectra for AA-AR-Hg^{2+} (a and c) and AA-AR (b and d)

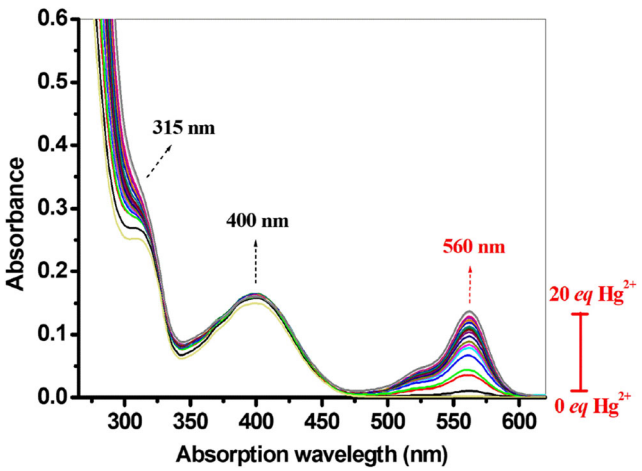

Fig. 3 UV–Vis. absorption spectra recorded for AA-AR at different Hg^{2+} concentrations Hg^{2+} concentration: 0.0–20.0 eq; AA-AR concentration: 10 μM

The fluorescence intensity of AA-AR-Hg^{2+} was set at 1.0 and the intensities of other species were normalized accordingly; Concentration of metal ion: 20 eq; Concentration of AA-AR: 10 μM; Excitation and emission wavelengths: $\lambda_{Ex}/\lambda_{Em}$ = 520 nm/592 nm.

As it is seen in the emission spectrum of AA-AR and the studied metal complexes of AA-AR (Fig. 4), 592 nm is a critical wavelength at which AA-AR emits light which is mostly specific to Hg^{2+} ion when excited at 520 nm. At the same excitation and emission wavelengths, most of the studied anions and cations did not induce a significant emission when compared to what Hg^{2+} ion did. Among the studied metal cations, Cu^{2+} and Al^{3+} exhibited somehow emissions when interacted with the probe AA-AR. However, the fluorescence emission intensity observed with Hg^{2+} was approximately 4–8 times greater than that we observed with these cations. Despite a somehow

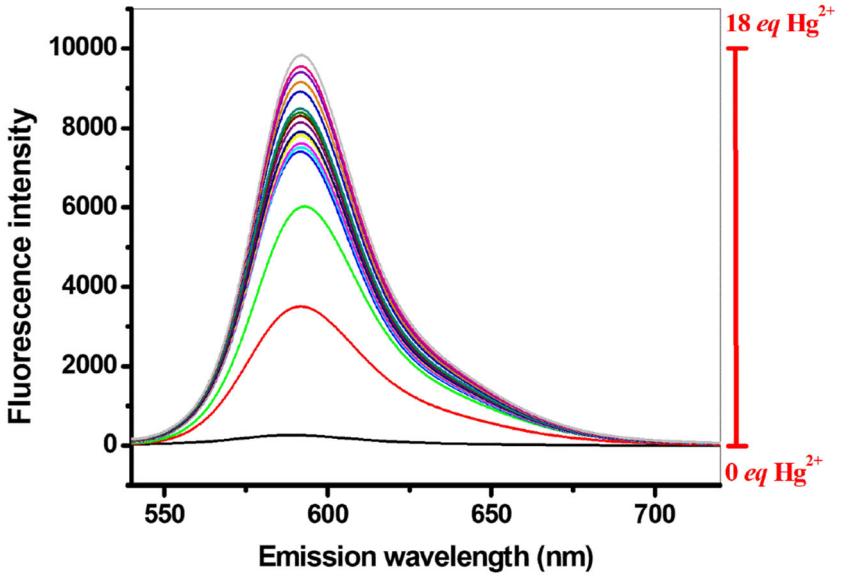

Fig. 4 Emission spectra recorded for AA-AR at different Hg^{2+} concentrations Hg^{2+} concentration: 0.0–18.0 eq; Concentration of AA-AR: 10 μM; $\lambda_{ex}/\lambda_{em}$ = 520 nm/592 nm

quenching effect of some anions (e.g. CN^- and HSO_4^-) on the emission of AA-AR, very similar results were obtained from the experiments conducted with anions. Hence, it was concluded that Hg^{2+} had an "overwhelming" fluorescence emission intensity among the studied ions, and the molecule was found to be fluorescing only in the presence of Hg^{2+}. This is a typical behavior observed with "*on-off*" sensing agents. Besides, the "*naked-eye*" detection was only achieved with Hg^{2+} ion, indicating a great selectivity toward this cation. Finally, owing to the observed efficient "*turn-on rate*", Hg^{2+} ion could be quickly detected under both (*i*) day-light and (*ii*) UV-light as is seen in Fig. 6.

The Impact of Coexisting Ions

As it is discussed above, the Hg^{2+}-sensing feature of AA-AR has been proven through single-solute experiments. However, the selectivity of a probe cannot be thoroughly evaluated on the basis of the results of single-solute experiments. This is true because the selectivity of a probe is reflected by its capability to discern the analyte in a mixture despite the presence of possible interferences that may come from matrix constituents. For this purpose, an AA-AR-Hg^{2+} solution, which contains 20 eq Hg^{2+}, was prepared and this solution was spiked with 20 eq of

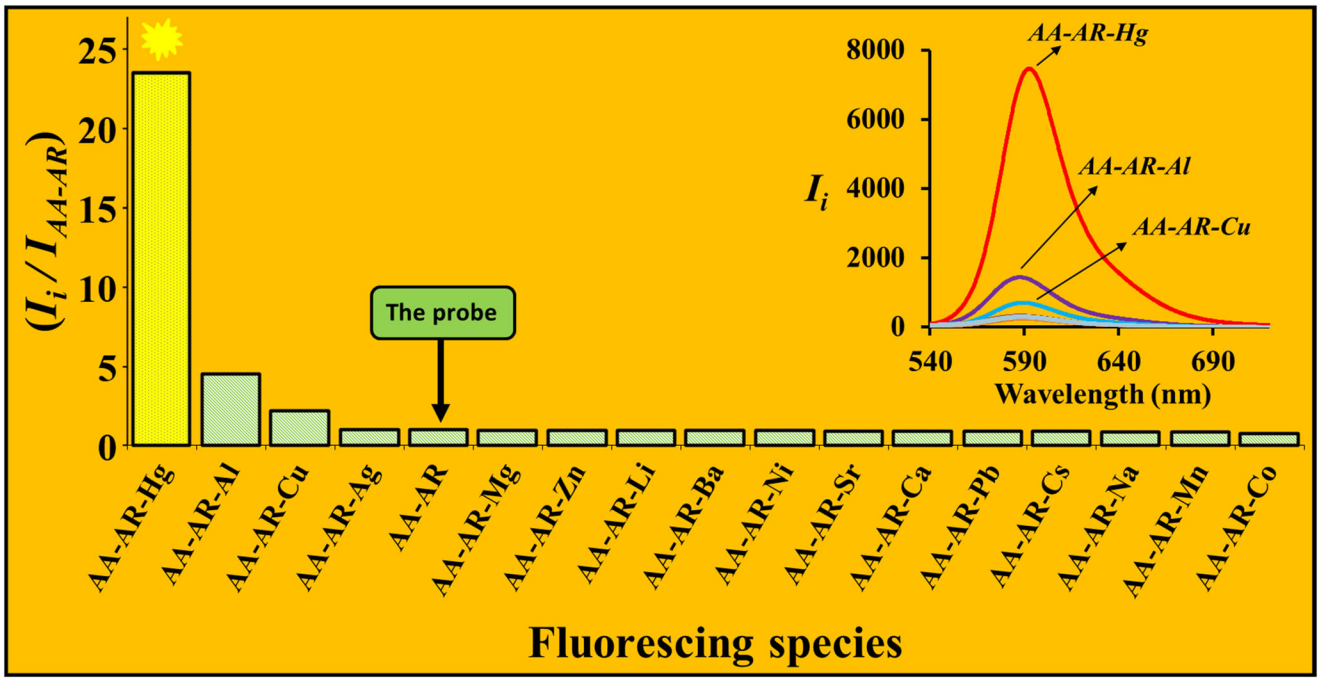

Fig. 5 Normalized fluorescence intensities for AA-AR and metal-interacted AA-AR

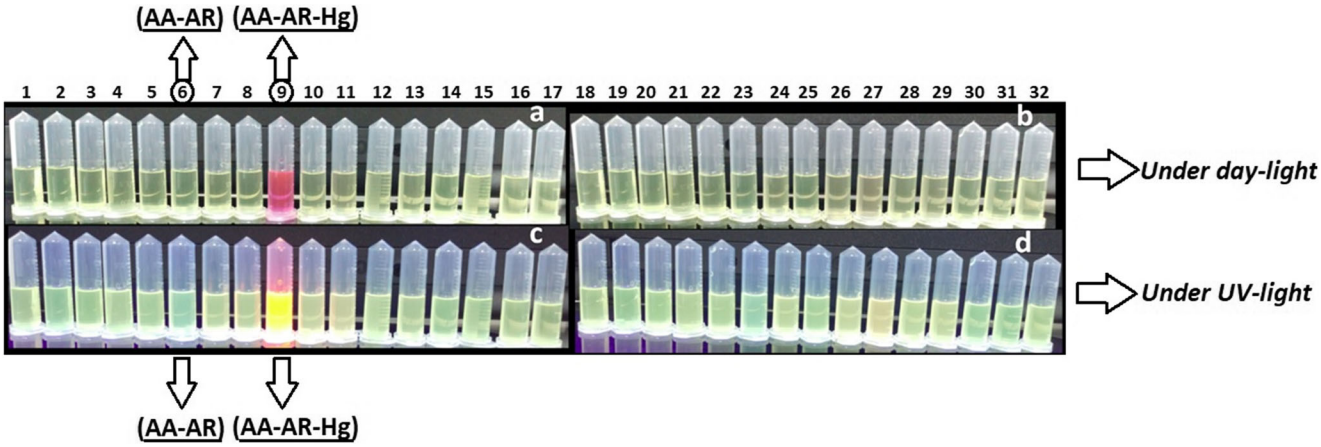

Fig. 6 The response of AA-AR to different ions under day-light (a and b) and UV-light (c and d) # Test tubes: (1) AA-AR + Li^+, (2) AA-AR + Na^+, (3) AA-AR + Ag^+, (4) AA-AR + Ca^{2+}, (5) AA-AR + Ba^{2+}, (6) AA-AR, (7) AA-AR + Co^{2+}, (8) AA-AR + Cs^+, (9) AA-AR + Hg^{2+}, (10) AA-AR + Cu^{2+}, (11) AA-AR + Mg^{2+}, (12) AA-AR + Mn^{2+}, (13) AA-AR + Pb^{2+}, (14) AA-AR + Ni^{2+}, (15) AA-AR + Sr^{2+}, (16) AA-AR + Zn^{2+}, (17) AA-AR + Al^{3+}, (18) AA-AR + Br^-, (19) AA-AR + Cl^-, (20) AA-AR + I^-, (21) AA-AR + HPO_4^{2-}, (22) AA-AR + $H_2PO_4^-$, (23) AA-AR + NO_3^-, (24) AA-AR + NO_2^-, (25) AA-AR + ClO_4^-, (26) AA-AR + AcO^-, (27) AA-AR + HSO_4^-, (28) AA-AR + SO_4^{2-}, (29) AA-AR + $Cr_2O_7^-$, (30) AA-AR + CO_3^{2-}, (31) AA-AR + OH^- and (32) AA-AR + HCO_3^-. Concentration of ions: 20 eq; Concentration of AA-AR: 10 μM; λ_{Ex}/ λ_{Em} = 520 nm/592 nm

different cations and/or anions. Fluorescence intensities of the final mixtures were measured at 520 nm (λ_{Ex})/592 nm (λ_{Em}) and graphed against the type of mixtures (Figs. 7 and 8). As is seen in Fig. 7, almost all the studied metal cations did not have a significant effect on the emission signal of AA-AR-Hg^{2+} complex except some metal cations (i.e. Al^{3+}, Cu^{2+}, and Li^+). As for the studied anions (Fig. 8), some of them (i.e. NO_2^-, CN^-, Br^-, $H_2PO_4^-$, SCN^-, and I^-) were found to have greater quenching effects on the fluorescence intensity of the complex AA-AR-Hg^{2+}. Nevertheless, the synthesized probe, i.e. AA-AR, was found to exhibit a nice Hg^{2+}-sensing property among many different cations and anions.

Possible Interaction Mechanism

Spectroscopic results given in previous sections supported the fast interaction capability of AA-AR with Hg^{2+} ion. According to the results, Hg^{2+} binding to AA-AR was evaluated as a process that is basically governed by a ring-opening reaction of spirolactam moiety in AA-AR. The process was found to be resulting in a net color change. Hg^{2+} binding to AA-AR was supported by the recorded UV-Vis. spectra (Fig. 3) so that the absorption band at around 560 nm was observed only in the case of AA-AR-Hg^{2+}. The absorption intensity at this wavelength was found to be increasing with increasing Hg^{2+} concentration from 0 to 20 eq, and further increments in

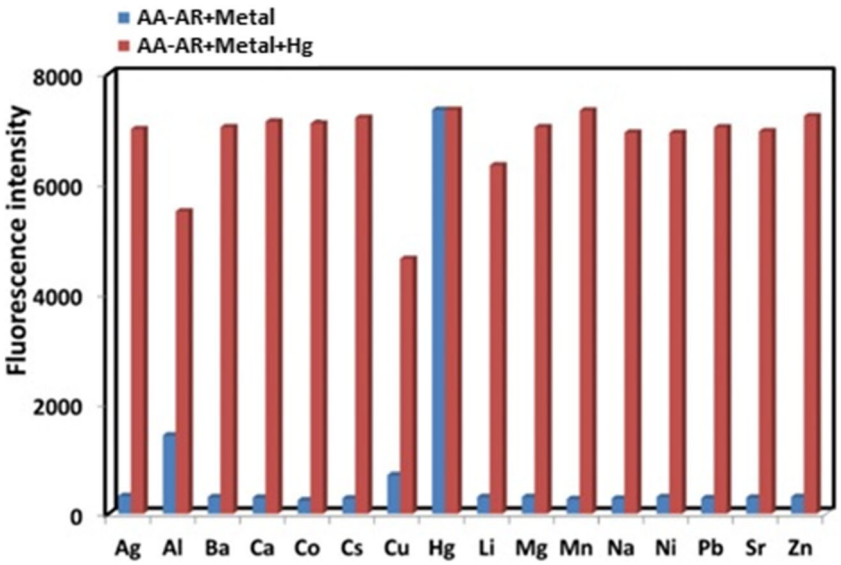

Fig. 7 The effect of interfering metal cations on the fluorescence intensity of AA-AR-Hg^{2+}. Concentration of interfering cation and Hg^{2+}: 20 eq; Concentration of AA-AR: 10 μM; λ_{Ex}/ λ_{Em} = 520 nm/592 nm

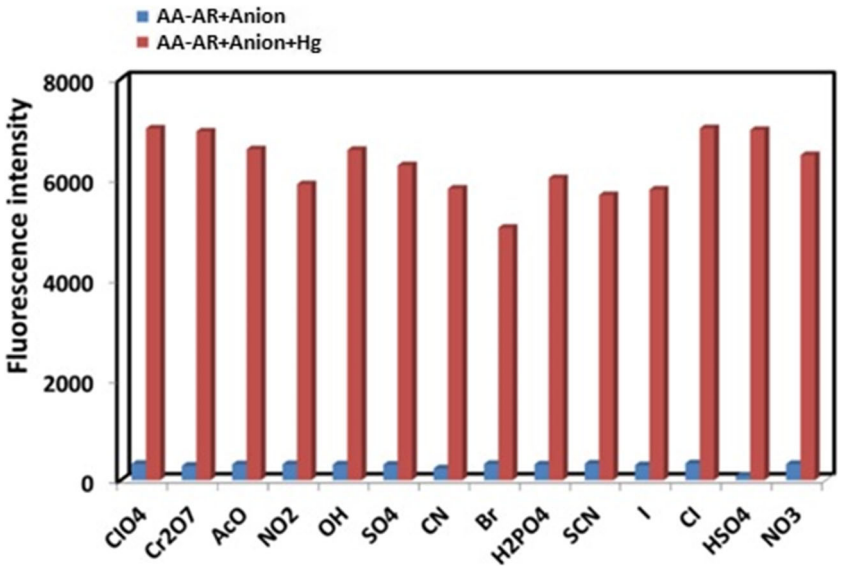

Fig. 8 The effect of interfering anions on the fluorescence intensity of AA-AR-Hg^{2+}. Concentration of interfering anion and Hg^{2+}: 20 eq; Concentration of AA-AR: 10 μM; $\lambda_{Ex}/\lambda_{Em}$ = 520 nm/592 nm

concentration did not cause further changes in the spectrum. Likewise, the absorption intensities at 315 and 400 nm tended to increase gradually, indicating a possible role of intra-ligand $\pi-\pi^*$ transitions [23]. Very similar results were observed with the fluorescence emission spectrum of AA-AR (Fig. 4) so that the band at 592 nm was arisen in the spectrum only after interacting AA-AR with Hg^{2+} ion. The fluorescence intensity at this wavelength was found to be increased gradually when the AA-AR solution was titrated with Hg^{2+}. The obtained data were used to calculate the detection limit for Hg^{2+} and found as 0.87 μM for the linear signal to the concentration range. This value is lower than (or comparable to) those obtained with some Hg^{2+}-selective chemosensors [23]. Moreover, the detection limit achieved with AA-AR for Hg^{2+} was found to be approximately 60 times less than that achieved with another rhodamine-based sensor prepared through a Schiff base-type reaction between rhodamine and quinoline-2-aldehyde [24]. Better sensitivity observed in the case of AA-AR is attributed to higher conjugation in the case of anthracene (compared to quinoline). Finally, when the spectral patterns of these two sensors compared, a bathochromic shift was obvious in the case of AA-AR. Hence, AA-AR exhibited excellent sensor properties for Hg^{2+} detection, and this led to fast Hg^{2+} detection even at sub-micromolar concentration levels.

The results obtained from UV-Vis and fluorescence spectroscopy analyses were, also, used to estimate the progress of Hg^{2+} coordination by AA-AR as well as the stoichiometry of the reaction. For this purpose, the recorded spectra were analyzed on the basis of the Job's plot method [25] and the Benesi-Hildebrand method [26, 27] (figures not shown). Both the methods evidenced a 1:1 stoichiometry for mercury complexation by AA-AR. Besides, from the Benesi-Hildebrand plot ($r^2 = 0.983$), the binding constant was calculated as 2.4×10^5 M^{-1}. Such a high binding constant might indicate the presence of a high affinity between AA-AR and Hg^{2+}. To have further information about the mechanism of Hg^{2+} binding, FTIR and NMR spectra were analyzed.

FTIR analyses (Fig. 1) confirmed the results of UV-Vis. spectroscopy analyses. For example, a strong band appeared at around 1631 cm^{-1} in the spectrum of AA-AR shifted to a lower frequency at 1608 cm^{-1} when AA-AR has interacted with Hg^2. This band is attributed to the azomethine group, and the spectral shift indicates the possible role of imine functionality in the mercury complexation process. Furthermore, a band related to the carbonyl group in the FTIR spectrum of AA-AR (at around 1683 cm^{-1}) was disappeared when it was interacted with Hg^{2+}, revealing the contribution of the carbonyl group in complexation. Another indication about the role of a possible spirolactam ring-opening reaction was a new band arisen at 1585 cm^{-1} in the spectrum of AA-AR after binding of Hg^{2+}, which is consistent with the previous findings in the literature [28].

Much more details about the complexation mechanism were obtained from the NMR titration experiments performed with an AA-AR solution in DMSO-d_6. For this purpose, 1.0 eq Hg^{2+} was added to this solution, and ^{1}H-NMR and ^{13}C-NMR analyses were conducted for the complex AA-AR-Hg^{2+}. As is seen in Fig. 2, the signal ascribed to imine proton at 8.31 ppm shifts to 8.60 ppm in the case of AA-AR-Hg^{2+} complex. This behavior is most probably due to the deshielding of azomethine group after the complexation of Hg^{2+} with AA-AR. Furthermore, the signals attributed to benzene protons were observed to be broadened upon the addition of Hg^{2+} ion, and this was attributed to the ring-opening reaction of spirolactam moiety. The results of ^{13}C-NMR supported this phenomenon so that a characteristic peak appeared (at 65.82 ppm) in the spectrum of AA-AR shifted to 142.6 ppm

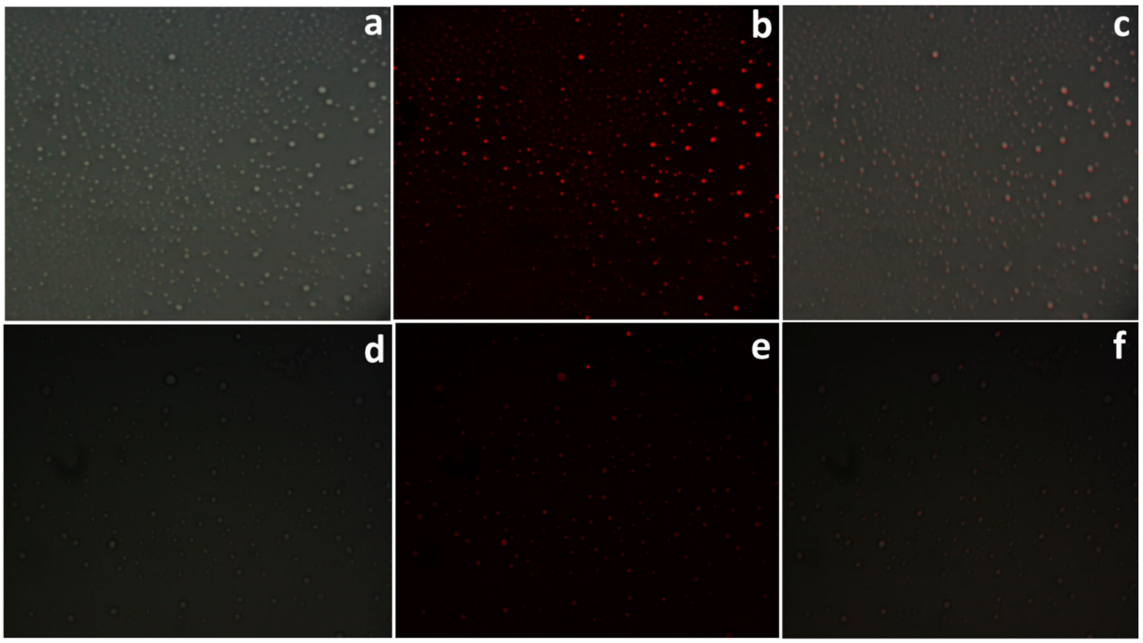

Fig. 9 Bright-field and fluorescence images recorded for MIA PaCa-2 and MCF7 living cells (a) Bright-field image of MIA PaCa-2 cell incubated with AA-AR and Hg^{2+}; (b) Fluorescence image of MIA PaCa-2 cells treated with AA-AR and Hg^{2+}; (c) Merged image of (a) and (b); (d) Bright-field image of MCF7 cells treated with AA-AR and Hg^{2+}; (e) Fluorescence image of MCF7 cells treated with AA-AR and Hg^{2+}; (d); (f) Merged image of (d) and (e). Concentration of Hg^{2+}: 0.010 mM; Concentration of AA-AR: 0.020 mM

in the case of AA-AR-Hg^{2+} complex (Fig. 2). Very similar results have been reported in previous studies [29]. Thus, the observed color change upon formation of the AA-AR-Hg^{2+} complex was ascribed to a ring-opening reaction of spirolactam moiety in the rhodamine framework.

Cell-Imaging

Owing to the accumulation of mercury ions in plants, animals, and microorganisms [2], the design and synthesis of new chemosensors for the detection of mercury ions in biological samples are deemed important. Therefore, a simple experiment was organized whereby Hg^{2+} ions are allowed to penetrate through living-cells (i.e. MCF7 and MIA PaCa-2), and afterward, the probe, AA-AR, was used to detect Hg^{2+} and thus to record cell images in a biological sample by a fluorescence microscope. In fluorescence images (Fig. 9), Hg^{2+}-smeared zones within the cells were visualized as bright fields after the addition of the AA-AR probe to the medium. Thus, Hg^{2+} stains in living cells could be detected by using a very dilute AA-AR solution (i.e. 20 μM), and thus the performance of the probe AA-AR was proven by detecting this toxic metal ion in living cells. At this point, the role of anthracene moiety in penetration of AA-AR through the cell membranes should be mentioned. This hydrophobic moiety is believed to facilitate penetration of the probe, which is water-soluble, through the lipid membranes of cells having hydrophobic character [30]. Hence, both receptor (i.e. anthracene) and fluorophore (i.e. rhodamine) parts of the newly designed sensor, AA-AR, were observed to be functioning in an expected way. This conclusion proves the successful design and synthesis of AA-AR.

Conclusions

In conclusion, a low-cost and efficient fluorescent probe (i.e. AA-AR) containing rhodamine and anthracene units has been developed for the first time. The probe exhibited excellent selectivity and sensitivity towards a toxic and mutagenic metal ion, Hg^{2+}, over various metal ions and anions. AA-AR exhibited a prominent Hg^{2+}-induced fluorescence response followed by an apparent color change under both day-light and UV-light. For example, under day-light, a net color change from light yellow to pink made a naked-eye detection possible for Hg^{2+}. The determination of Hg^{2+} in aqueous samples was found to be possible even at trace levels. The emission signals were found to be useful to detect Hg^{2+} at trace concentration levels with a detection limit of 8.73×10^{-7} M. Finally, the probe, which was synthesized in a new manner based on a facile Schiff-base type reaction, exhibited good penetrating performance through the cell membranes and thus it was successfully utilized in intracellular mercury detection and imaging. Thus, the reaction protocol presented here offers a straightforward and sulfur-free (and thus environmentally-friendly) manner for the design and synthesis of Hg^{2+}-selective probes.

Acknowledgments Authors wish to thank Karamanoglu Mehmetbey University (Karaman, Turkey), and Nigde Ömer Halisdemir University (Nigde, Turkey) for the facilities provided.

References

1. Kim D-H, Seong J, Lee H, Lee K-H (2014) Ratiometric fluorescence detection of Hg(II) in aqueous solutions at physiological pH and live cells with a chemosensor based on tyrosine. Sensors Actuators B Chem 196:421–428. https://doi.org/10.1016/j.snb.2014.02.029
2. Nolan EM, Lippard SJ (2008) Tools and tactics for the optical detection of mercuric ion. Chem Rev 108:3443–3480. https://doi.org/10.1021/cr068000q
3. Kim HN, Ren WX, Kim JS, Yoon J (2012) Fluorescent and colorimetric sensors for detection of lead, cadmium, and mercury ions. Chem Soc Rev 41:3210–3244. https://doi.org/10.1039/C1CS15245A
4. Zhang X, Xiao Y, Qian X (2008) A Ratiometric fluorescent probe based on FRET for imaging Hg 2+ ions in living cells. Angew Chemie Int Ed 47:8025–8029. https://doi.org/10.1002/anie.200803246
5. Jiang J, Liu W, Cheng J, Yang L, Jiang H, Bai D, Liu W (2012) A sensitive colorimetric and ratiometric fluorescent probe for mercury species in aqueous solution and living cells. Chem Commun 48:8371–8373. https://doi.org/10.1039/c2cc32867d
6. Taki M, Akaoka K, Iyoshi S, Yamamoto Y (2012) Rosamine-based fluorescent sensor with Femtomolar affinity for the reversible detection of a mercury ion. Inorg Chem 51:13075–13077. https://doi.org/10.1021/ic301822r
7. Quang DT, Wu J-S, Luyen ND et al (2011) Rhodamine-derived Schiff base for the selective determination of mercuric ions in water media. Spectrochim Acta Part A Mol Biomol Spectrosc 78:753–756. https://doi.org/10.1016/j.saa.2010.12.010
8. Wolfe MF, Schwarzbach S, Sulaiman RA (1998) Effects of mercury on wildlife: a comprehensive review. Environ Toxicol Chem 17:146–160. https://doi.org/10.1002/etc.5620170203
9. Su W, Yang B (2013) Novel highly selective fluorescent chemosensors for Hg(II). Chem Res Chinese Univ 29:657–662. https://doi.org/10.1007/s40242-013-2363-9
10. Nuriman KB, Verboom W (2009) Selective chemosensor for Hg(II) ions based on tris[2-(4-phenyldiazenyl)phenylaminoethoxy]cyclotriveratrylene in aqueous samples. Anal Chim Acta 655:75–79. https://doi.org/10.1016/j.aca.2009.09.045
11. Ghanei-Motlagh M, Taher MA, Heydari A et al (2016) A novel voltammetric sensor for sensitive detection of mercury(II) ions using glassy carbon electrode modified with graphene-based ion imprinted polymer. Mater Sci Eng C 63:367–375. https://doi.org/10.1016/j.msec.2016.03.005
12. Detcheva A, Grobecker KH (2006) Determination of Hg, Cd, Mn, Pb and Sn in seafood by solid sampling Zeeman atomic absorption spectrometry. Spectrochim Acta Part B At Spectrosc 61:454–459. https://doi.org/10.1016/j.sab.2006.03.016
13. Gao Y, De Galan S, De Brauwere A et al (2010) Mercury speciation in hair by headspace injection–gas chromatography–atomic fluorescence spectrometry (methylmercury) and combustion-atomic absorption spectrometry (total Hg). Talanta 82:1919–1923. https://doi.org/10.1016/j.talanta.2010.08.012
14. Alizadeh T, Hamidi N, Ganjali MR, Rafiei F (2018) Determination of subnanomolar levels of mercury (II) by using a graphite paste electrode modified with MWCNTs and Hg(II)-imprinted polymer nanoparticles. Microchim Acta 185:16–19. https://doi.org/10.1007/s00604-017-2534-3
15. Kavitha R, Stalin T (2014) A highly selective chemosensor for colorimetric detection of Hg2+ and fluorescence detection of pH changes in aqueous solution. J Lumin 149:12–18. https://doi.org/10.1016/j.jlumin.2013.11.044
16. Ni J, Li Q, Li B, Zhang L (2013) A novel fluorescent probe based on rhodamine B derivative for highly selective and sensitive detection of mercury(II) ion in aqueous solution. Sensors Actuators B Chem 186:278–285. https://doi.org/10.1016/j.snb.2013.06.011
17. Kim HN, Lee MH, Kim HJ, Kim JS, Yoon J (2008) A new trend in rhodamine-based chemosensors: application of spirolactam ring-opening to sensing ions. Chem Soc Rev 37:1465–1472. https://doi.org/10.1039/b802497a
18. Tantipanjaporn A, Prabpai S, Suksen K, Kongsaeree P (2018) A thiourea-appended rhodamine chemodosimeter for mercury(II) and its bioimaging application. Spectrochim Acta Part A Mol Biomol Spectrosc 192:101–107. https://doi.org/10.1016/j.saa.2017.10.057
19. Hong M, Lu S, Lv F, Xu D (2016) A novel facilely prepared rhodamine-based Hg2+ fluorescent probe with three thiourea receptors. Dyes Pigments 127:94–99. https://doi.org/10.1016/j.dyepig.2015.12.023
20. Wu J-S, Hwang I-C, Kim KS, Kim JS (2007) Rhodamine-based Hg2+ -selective Chemodosimeter in aqueous solution: fluorescent OFF−ON. Org Lett 9:907–910. https://doi.org/10.1021/ol070109c
21. Fang Y, Li X, Li J-Y et al (2018) Thiooxo-Rhodamine B hydrazone derivatives bearing bithiophene group as fluorescent chemosensors for detecting mercury(II) in aqueous media and living HeLa cells. Sensors Actuators B Chem 255:1182–1190. https://doi.org/10.1016/j.snb.2017.06.050
22. Chen X, Meng X, Wang S et al (2013) A rhodamine-based fluorescent probe for detecting Hg2+ in a fully aqueous environment. Dalt Trans 42:14819–14825. https://doi.org/10.1039/c3dt51279g
23. Wang C, Lam H-C, Zhu N, Wong KM-C (2015) Introduction of luminescent rhenium(I), ruthenium(II), iridium(III) and rhodium(III) systems into rhodamine-tethered ligands for the construction of bichromophoric chemosensors. Dalt Trans 44:15250–15263. https://doi.org/10.1039/C5DT00661A
24. Saha S, Mahato P, G UR, et al (2012) Recognition of Hg 2+ and Cr 3+ in physiological conditions by a Rhodamine derivative and its application as a reagent for cell-imaging studies. Inorg Chem 51:336–345. https://doi.org/10.1021/ic2017243
25. Job P (1928) Formation and stability of inorganic complexes in solution. Ann di Chim Appl 9:113–203
26. Benesi HA, Hildebrand JH (1949) A spectrophotometric investigation of the interaction of iodine with aromatic hydrocarbons. J Am Chem Soc 71:2703–2707. https://doi.org/10.1021/ja01176a030
27. Kim HM, Jung C, Kim BR et al (2007) Environment-sensitive two-photon probe for intracellular free magnesium ions in live tissue. Angew Chemie Int Ed 46:3460–3463. https://doi.org/10.1002/anie.200700169
28. Ku K-S, Hwang J-Y, Muthukumar P, Son Y-A (2016) A novel fluorescent Chemosensor based on β-(2-Pyridyl)acrolein-Rhodamine B derivative: polymer particle interaction with an enhanced sensing performance. KONA Powder Part J 33:228–238. https://doi.org/10.14356/kona.2016003
29. Li H, Guan H, Duan X, Hu J, Wang G, Wang Q (2013) An acid catalyzed reversible ring-opening/ring-closure reaction involving a cyano-rhodamine spirolactam. Org Biomol Chem 11:1805–1809. https://doi.org/10.1039/c3ob27356c
30. Takeuchi T, Kosuge M, Tadokoro A, Sugiura Y, Nishi M, Kawata M, Sakai N, Matile S, Futaki S (2006) Direct and rapid cytosolic delivery using cell-penetrating peptides mediated by Pyrenebutyrate. ACS Chem Biol 1:299–303. https://doi.org/10.1021/cb600127m